Remote Sensing in Ecology and Conservation
Open Access
ZSL LET'S WORK FOR WILDLIFE

ORIGINAL RESEARCH

From ecology to remote sensing: using animals to map land cover

Ruben Remelgado[1,2], Kamran Safi[3] & Martin Wegmann[1]

[1]Department of Remote Sensing, Institute of Geography and Geology, Oswald Kuelpe Weg 86, Wuerzburg 97074,Germany
[2]Macroecology and Society lab, German Centre for Integrative Biodiversity Research (iDiv) Halle-Jena-Leipzig, Leipzig, Saxony, Germany
[3]Department of Migration, Max Planck Institute of Animal Behavior, Am Obstberg 1, Radofzell 78315, Germany

Keywords
Animal Tracking, land cover, land use, movement ecology, R, remote sensing

Correspondence
Ruben Remelgado, German Centre for Integrative Biodiversity Research (iDiv) Halle-Jena-Leipzig, Ringgold standard institution - Macroecology and Society lab, Deutsche Platz 4, Leipzig, Saxony 04103, Germany.
Tel: +49 341 9733244; E-mail: ruben.remelgado@idiv.de

Editor: Ned Horning
Associate Editor: Abdulhakim Abdi

Received: 4 December 2018; Revised: 29 July 2019; Accepted: 12 August 2019

doi: 10.1002/rse2.126

Remote Sensing in Ecology and Conservation 2020;**6** (1):93–104

Abstract

Land cover is a key variable in monitoring applications and new processing technologies made deriving this information easier. Yet, classification algorithms remain dependent on samples collected on the field and field campaigns are limited by financial, infrastructural and political boundaries. Here, animal tracking data could be an asset. Looking at the land cover dependencies of animal behaviour, we can obtain land cover samples over places that are difficult to access. Following this premise, we evaluated the potential of animal movement data to map land cover. Specifically, we used 13 White Storks (*Cicona cicona*) individuals of the same population to map agriculture within three test regions distributed along their migratory track. The White Stork has adapted to foraging over agricultural lands, making it an ideal source of samples to map this land use. We applied a presence–absence modelling approach over a Normalized Difference Vegetation Index (NDVI) time series and validated our classifications, with high-resolution land cover information. Our results suggest White Stork movement is useful to map agriculture, however, we identified some limitations. We achieved high accuracies (F1-scores > 0.8) for two test regions, but observed poor results over one region. This can be explained by differences in land management practices. The animals preferred agriculture in every test region, but our data showed a biased distribution of training samples between irrigated and non-irrigated land. When both options occurred, the animals disregarded non-irrigated land leading to its misclassification as non-agriculture. Additionally, we found difference between the GPS observation dates and the harvest times for non-irrigated crops. Given the White Stork takes advantage of managed land to search for prey, the inactivity of these fields was the likely culprit of their underrepresentation. Including more species attracted to agriculture – with other land-use dependencies and observation times – can contribute to better results in similar applications.

Introduction

Land cover mapping is one of the main applications of remote sensing and a clear requirement of environmental monitoring initiatives. Among others, land cover is essential in climate change mitigation (Dirmeyer et al. 2010; Kalacska et al. 2017), habitat management (Lang et al. 2015; Lucas et al. 2015; Vaz et al. 2015) and food security monitoring (Verburg et al. 2013; Whitcraft et al. 2015; Brown 2016), demanding its regular update in a consistent and systematic manner (Wulder et al. 2018).

The increase in the number of satellite missions over the recent decades has made this possible. Since the first Landsat mission was launched in 1972, several new multispectral satellite missions have helped refine land cover information. Through dense time series of satellite images, these missions reveal subtle but relevant differences among land cover types (Zhao et al. 2016; Yin et al.

© 2019 The Authors. *Remote Sensing in Ecology and Conservation* published by John Wiley & Sons Ltd on behalf of Zoological Society of London. This is an open access article under the terms of the Creative Commons Attribution-NonCommercial License, which permits use, distribution and reproduction in any medium, provided the original work is properly cited and is not used for commercial purposes.

2018), and help map land cover change (Hansen and Loveland 2012; Tewkesbury et al. 2015). Moreover, the rapid development of processing technologies as greatly advanced land cover mapping. As initially shown by Hansen et al. (2013) and extended by several other authors (Dong et al. 2016; Shelestov et al. 2017; Xiong et al. 2017; Liu et al. 2018), the access to high-performance computing platforms such as Google Earth Engine (GEE) offers an important stepping stone. It supports the rapid processing of satellite data thus creating the basis for the timely and consistent mapping of land cover on a global scale and with increasingly finer spatial resolutions (Shelestov et al. 2017).

Yet, while the access to data and processing capabilities made land cover mapping easier, we are still faced with basic challenges. Even if we brush aside the data quality issues created by elements such as atmospheric conditions (e.g. clouds, shadows) and topographic effects (e.g. illumination differences), the collection of training samples remains a big concern. To translate satellite data into land cover, we require representative samples that account for the spectral, spatial and temporal variability in different land cover classes (Foody 2002). And, as shown by previous research, the quality of these samples drives the quality of a land cover classification (Foody 2004; Hansen and Loveland 2012).

When dealing with large-scale applications, collecting a sufficient number of representative samples is a difficult task. It is true that the development of automated sampling approaches has made this task easier (Knorn et al. 2009; Jia et al. 2014; Radoux et al. 2014; Mack et al. 2017). However, such innovations still depend on quality, ground-truth data collected through image interpretation and field surveys, a process with its own challenges.

First, distinguishing land cover types from satellite imagery alone can be difficult. For example if our aim is to distinguish crop types, we require very high-resolution satellite imagery with a low temporal resolution – such as the ones provided by Google Earth – to deal with complex land-use patterns (e.g. mixed crops). However, perceiving differences in crop types is not always possible with a low temporal resolution. Due to practices such as crop rotation, contrasts in cultivation patterns do not always translate into different crop types. Additionally, different crop types can have similar visual properties (e.g. texture, colour), which makes it difficult to distinguish them remotely.

Second, field surveys are sometimes impractical. Visiting sampling sites assures a reasonable level of certainty that image interpretation cannot. However, designing a sampling scheme sensitive to the dangers of spatial autocorrelation (Wulder and Boots 1998; Griffith and Chun 2016) can become costly due to its potentially broad spatial coverage. Moreover, some locations are difficult to access. According to the Global Accessibility map developed by the Joint Research Center (JRC) which shows the required travel time from each pixel to the nearest city with more than 50 000 inhabitants (Weiss et al. 2018), roughly 30% of the earth's land surface requires over 1 day of travel to be reached by land or water. This of course does not account for the difficult mobility over areas with dense vegetation (e.g. tropical forests) or adverse climate conditions (e.g. deserts), making this number potentially larger. Additionally, the access to some areas is constrained due to political and social instability. According to the Armed Conflict Location & Event Data Project (ACLED), in Africa alone, 2018 registered more than 3000 violent conflicts and over 7000 fatalities over 42 countries (Raleigh et al. 2010), making it difficult to access a large portion of the continent safely. Such limitations also constrain novel, human-based sampling methods such as crowdsourcing, where scientists rely on motivated individuals to collect data (See et al. 2015; Fritz et al. 2017; Brovelli et al. 2018).

Considering the limitations of automated and human-based sampling methods, we wondered: why not use animals to collect data on land cover? In the scope of animal movement research, Geographic Positioning System (GPS) tracking technologies have evolved impressively. The spatial error of a tracking device can now be measured in a few metres and the inclusion of solar power technologies allowed for the consistent, long-term monitoring of animal behaviour. And, as we observe the behaviour of an animal, we also collect information on its environmental drivers (Avgar et al. 2013; Dodge et al. 2014; van Toor et al. 2016). Behaviours such as resting and foraging have specific environmental requirements (Péron et al. 2016; Abrahms et al. 2017) that can potentially be translated into land cover classes. However, while the relationship between movement and land cover has been roughly explored (Da Silveira et al. 2016; Brown et al. 2017; Rickbeil et al. 2017), this premise has not been tested for the purpose of land cover mapping.

Our paper tackles this knowledge gap with high-resolution animal tracking data from a White Stork (*Cicona cicona*) population. The White Stork is a bird species that has adapted to foraging over agriculture land (Van Den Bossche 2002) and it takes advantage of management practices such as grassland grazing and crop harvesting to find preys that feed on crops (e.g. small rodents). As a consequence, we ask two important questions: 1) *Can we use White Stork tracking data to map agriculture?*, 2) *Can we map agriculture consistently in space using this data?* To answer these questions, we applied a presence–absence classification approach to map agriculture over 3 study regions with different land-use practices and compared

 © 2019 The Authors. *Remote Sensing in Ecology and Conservation* published by John Wiley & Sons Ltd on behalf of Zoological Society of London.

the output against high-resolution, ground-truth information on land cover (question 1). Our test regions were distributed along the migratory track of the White Stork population, allowing us to evaluate the spatial consistency of our mapping approach (question 2).

Materials and Methods

Study regions

We selected 3 study regions along the migratory track of the White Stork individuals used in this study (Fig. 1). These regions are located between Germany and Switzerland (referred hereon as R1), between France and Spain (referred hereon as R2) and in Southern Spain (referred hereon as R3). The test regions have areas between 3100 km^2 and 4300 km^2 and are all intensively managed. According to the CORINE Land Cover (CLC) for 2012 (European Environment Agency (EEA), 2019), within each study region, more than 40% of the area is occupied by agriculture. The percentage of non-managed vegetation varies between 24 and 44% and is mostly composed by forest, shrubs and grasslands. Wetlands are nearly inexistent with less than 1% of the area in all study regions. Areas with little or no vegetation (e.g. rocks, bare ground), urban areas and within-land water bodies account for less than 15%. The main difference between study regions is the type of agriculture management. While the agricultural land in all regions have non-irrigated arable land (28-59%), R1 has no irrigated land, whereas R2 and R3 have 38% and 39% respectively. Moreover, R1 has a higher proportion of permanent crops (37% against 2 and 6%) and R2 and R3 have a higher percentage of pastures (15 and 25% against 4%).

Remote sensing data processing

Our goal was to map agriculture within different regions and compare the accuracy of our results. Thus, we aimed for environmental variables that: 1) are sensitive to management; 2) are transferrable and comparable among test regions. Following this premise, for each of the test regions, we derived time series of 16-day Normalized Difference Vegetation indices (NDVI) with a resolution of 232 m. To derive this time series, we used collection 6 data of MOD13Q1 (Didan 2015a) MYD13Q1 (Didan 2015b), derived from MODIS Terra and Aqua, respectively, which provides pre-calculated NDVI. We masked each NDVI layer using the highest quality flags, stacked both products and linearly interpolated missing values accounting for the Day of Acquisition (DoA). For each pixel, we interpolated a missing value if the temporal distance between the following and previous pixels was lower than 2 months. This threshold was empirically defined to avoid generalizing the phenological curve described by the NDVI when dealing with large data gaps. We calculated these data for the year of 2013, which coincides with the year the animals were tagged and monitored (see section 2.3). Then, we smoothed the interpolated time series using a median filter and sorted the final output from the smallest to the highest NDVI value to generalize our time series. The White Stork is attracted to recently planted and harvest crops and, as a consequence, we risked failing to capture the diversity of crop types in the different regions. Therefore, by generalizing the time series, movement-based samples (section 2.3) represented temporally dynamic pixels – related to agriculture –rather than crop-specific temporal curves. Due to the persistence of missing data between January and March and between October and December – related to cloud cover – we decided to exclude the images from these months. The output was a stack of 12 NDVI images for each study region. The code used to derive the NDVI time series can be found in section 1 of the Appendix 1.

Animal movement data processing

The White Stork is an iconic species that takes advantage of human settlements. Areas dominated by agriculture attract, for example small birds and mammals on which the White Stork preys upon leading the species to consistently visit such environments (Fig. 2). Combined with its seasonal migration patterns (Flack et al. 2016), the relationship between the White Stork and humans makes it the ideal species to test the use of animal movement data to map agriculture. To achieve this, we derived presence samples (related to agriculture) and absence samples (not related to agriculture) using movement data from 13 White Storks juveniles from the same population (https://doi.org/10.5441/001/1.78152p3q).

The animals were tagged in Radozell, Germany, with solar-powered, high-resolution GPS devices with a temporal resolution of 5 min and a standard spatial error of 3.6 m. The first animal of this population was tracked on 26/06/13 and the movement dataset extends far beyond the year of 2013. However, we decided to constrain our sampling efforts to this year to avoid including samples related to land cover changes. Although the movement data consists of individuals of the same population, they had different migration periods. Thus, the study regions were visited at different dates. R1 was observed between 26/06 and 22/09, R2 between 12/08 and 09/09 and R3 between 18/08 and 20/10.

For each animal, we translated each coordinate pair in the tracking data into pixel positions within a grid with

© 2019 The Authors. *Remote Sensing in Ecology and Conservation* published by John Wiley & Sons Ltd on behalf of Zoological Society of London.

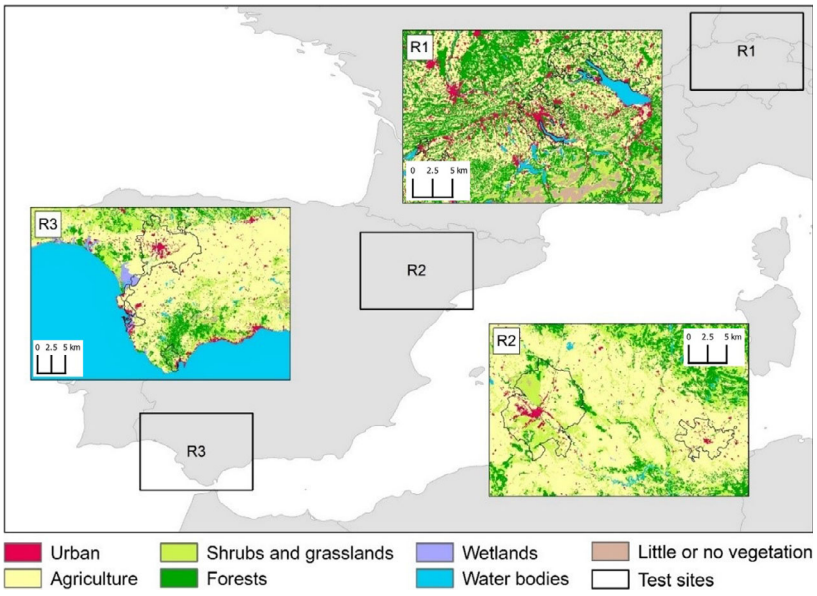

Figure 1. Location of the test sites and their land cover composition.

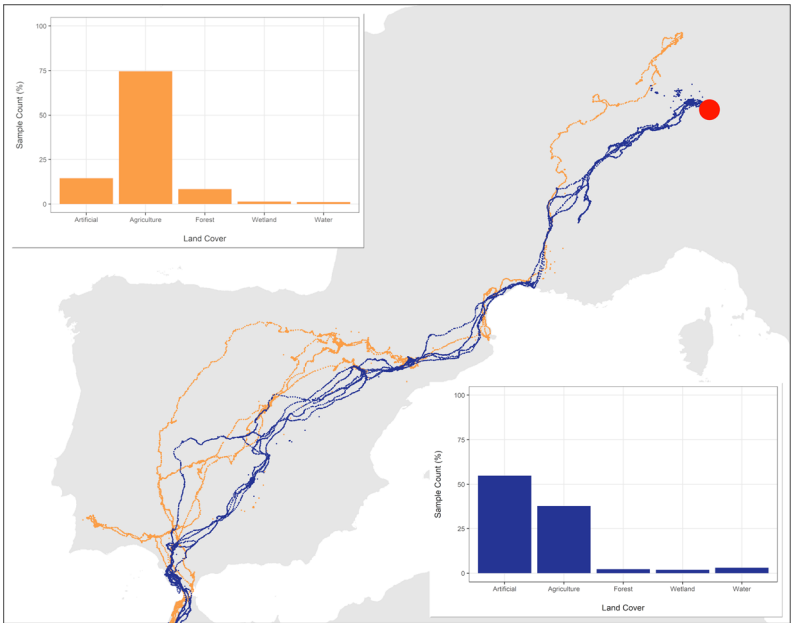

Figure 2. Relative distribution of movement data points per class based on the Corine Land Cover for 2012. The figure shows the winter (in blue) and summer (in orange) migration for all White Stork individuals considered in this study. Most points were registered over agriculture, suggesting the animals spent most of the recorded time within this land cover type. The red point marks the nesting site in R1 where the population was initially tagged.

the same extent and resolution as our NDVI time series (derived in section 2.2). On a daily basis, for each group of temporally consecutive observations within a pixel, we derived mean coordinates and reported the elapsed time in minutes. Then, we aggregated the samples of all individuals, estimated the maximum elapsed time per pixel and filtered-out pixels with zero time spent to remove redundant observations related to flyovers. By combining all individuals in this analysis, we preserved differences in resource selection among individuals. Finally, we filtered-out samples with an NDVI amplitude below 0.2 to focus on temporally dynamic pixels – likely related to agriculture – and remove those likely related to resting behaviour over non-agricultural land (e.g. buildings). The

© 2019 The Authors. *Remote Sensing in Ecology and Conservation* published by John Wiley & Sons Ltd on behalf of Zoological Society of London.

selected samples were taken as presences and assigned to each study region.

To select absences, we used the algorithm proposed in a recent paper (Remelgado et al. 2018). This algorithm identifies spatially connected groups of samples associated to presences and performs a Principle Components Analysis (PCA) over the environmental conditions associated to the sampled pixels – here described by the NDVI time series. Then, for each Principal Component (PC), the algorithm iterates through each group of spatially connected, sampled pixels and estimates the median and Median Absolute Deviation (MAD) of the variance. At each iteration, all samples outside of 1 MAD from the median are selected as potential absences and kept for further analysis. After iterating for all PC's, the algorithm identifies the pre-selected samples that were chosen in all PC iterations (Fig. 3). Those that fit that criteria are then returned as absences. The selection of absences was done separately for each study region. The code used to derive presences and absences can be found in the sections 2 and 3 of the Appendix 1.

Modelling and mapping of agriculture

For each study site, we used the NDVI time series derived in section 2.2. as predictors and the samples derived in section 2.3 as response variables to build a Random Forest (RF) model. We used the algorithm of Breiman (Breiman 2001) implemented in the R package *randomForest* (Liaw and Wiener 2002). The output models were then used to map agriculture within the corresponding study regions. Finally, we smoothed the class 'Agriculture' in the resulting maps using a dilation and erosion filter with a 3 × 3 pixel window. This last step aimed to include misclassified agriculture pixels neighbouring correctly classified ones due to the lack of mixed pixels in the training data. These pixels are often related to, for example cropland-forest transition areas. The final output was a map of 'Agriculture' and 'Not Agriculture'. The code used for this classification can be found in the section 4 of the Appendix 1.

Validation

We validated the maps derived in section 2.4 with Urban Atlas (UA) data from the Copernicus Land Monitoring Services (European Environmental Agency, 2017). The UA provides manually vectorized land cover and land use (LULC) data with a minimum mapping unit of 0.25-1 ha, which was locally validated between 2012 and 2015 through field surveys. We aggregated the original class scheme into 'Not Agriculture' and 'Agriculture' (Table 1) to match our target classes. Moreover, we manually modified the class 'Industrial, commercial, public, military and private units' to include only buildings as this class combines vegetated and non-vegetated land covers.

For each class in the new class scheme, we identified the pixels covered by the corresponding polygons and, for each pixel, estimated the percent overlap which is defined by the ratio between the area of the pixel and the area of the polygon intersection. We filtered-out pixels that had a percent overlap lower than 75% to avoid biased accuracy results related to mixed-pixels.

Finally, we selected an equal amount of samples for 'Agriculture' and 'Not Agriculture' considering only polygons with a minimum mapping unit of 62 000 m^2 (i.e. 1

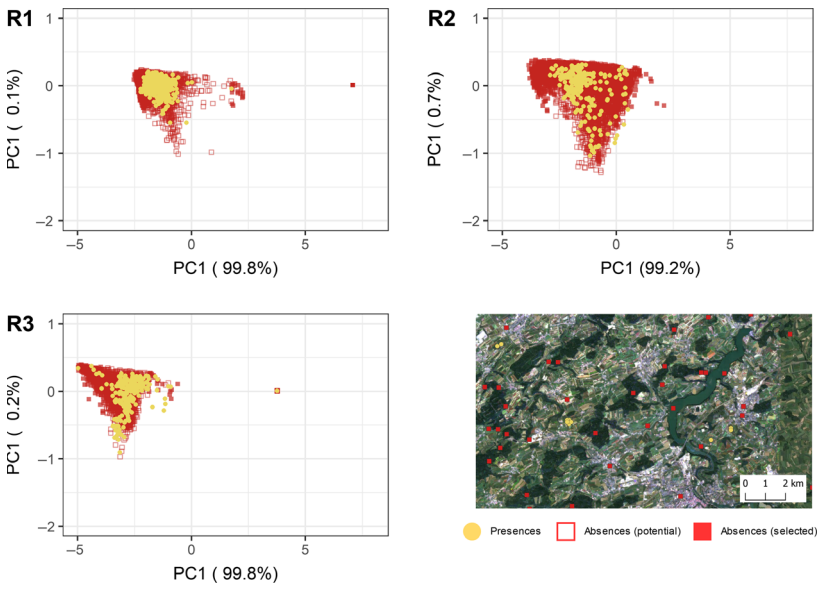

Figure 3. PCA results for R1, R2 and R3. On the bottom right, an example image extracted from R1 comparing the spatial distribution of presences and absences. The sample selection process identified absences over land cover types with very distinct NDVI profiles in comparison to agriculture (e.g. urban, water), but also over land cover transition zones (e.g. agriculture-forest) which are critical to determine the spectral boundaries of agricultural land.

© 2019 The Authors. *Remote Sensing in Ecology and Conservation* published by John Wiley & Sons Ltd on behalf of Zoological Society of London.

MODIS pixel). For each validation set, we chose 1000 samples composed by every associated class where the amount of samples per class equals their relative count within the total set of samples. This step made our validation scheme sensitive to the composition of the landscape assuring that dominant land cover types contributed more to the final accuracy. We reported the map accuracy with a F1-measure (Jäger and Benz 2000) for each validation set. The F1-measure is estimated as

$$F1 = 2 \cdot \frac{P \cdot R}{P + R}$$

where P is the Precision (ratio of true positives within the number of predicted values) and R is the Recall (ratio of true positives within the number of validation samples).

Results

Distribution of validation samples

We collected an equal number of samples (i.e. 1000) for 'Agriculture' and 'Not Agriculture' (Fig. 4) and their composition varied among study regions due to differences in land cover. In all cases, the class 'Agriculture' mostly consisted of 'Croplands' samples representing 42–50% of the original amount. Conversely, 'Permanent crops' were rare in all study regions and, consequently, the proportion of samples ranged between 0.01% and 2%. 'Grasslands' are unevenly distributed across study regions and are represented by less than 2% of samples in R2 and R3 and 6% in R1. As for the class 'Not Agriculture', the largest amount of samples fell within the class 'Little or no vegetation' in all study regions with 29–49%. Samples from other vegetated land cover classes such as 'Forests' were scarce with the exception of R1 where the proportion of validation samples for 'Forests' was of 19%. 'Wetlands' represented less than 1% of samples in all cases. Finally, looking at non vegetated classes, 'Urban (continuous)' and 'Urban (discontinuous)' were consistently rare with 1–2% of samples, whereas 'Water' was not represented, except R1 where this class contributed with 9% of samples.

Table 1. Conversion of the UA (Urban Atlas) class scheme.

Original	New	Aggregated
Continuous Urban Fabric (>80%)	Urban (Continuous)	Not Agriculture
Industrial, commercial, public, military and private units		
Discontinuous Urban Fabric (50–80%)	Urban (Discontinuous)	
Discontinuous Urban Fabric (30–50%)		
Discontinuous Urban Fabric (10–30%)		
Discontinuous Urban Fabric (<10%)		
Isolated Structures		
Sports And Leisure Facilities	Little or no vegetation	
Fast Transit Roads And Associated Land		
Railways And Associated Land		
Extraction And Dump Sites		
Construction Sites		
Forests		
Wetlands		
Water		
Pastures	Grasslands	Agriculture
Herbaceous Vegetation		
Arable Land		
Permanent Crops		

Model training and Map validation

Our predictive models were trained using 89–142 presence samples and 2722–5533 absence samples. The number of presence samples represents a loss of 54–82% of the amount of pixels covered by movement data before the removal of redundant and poor quality samples.

The model performances varied among study regions (Fig. 5) as did the spatial plausibility of the results (Fig. 6). The F1-scores were comparatively stable in R1 and R3 with a difference in accuracy between 'Agriculture' and 'Not Agriculture' of 0.02 and 0.04 respectively. The F1-scores for these study regions were of 0.79 and 0.82 for 'Agriculture' and 0.82 and 0.87 for 'Not Agriculture'. R2 performed comparatively worse with 0.2 for 'Agriculture' and 0.69 for 'Not Agriculture'.

Discussion

Our results extend on previous research on the link between animal behaviour and land cover taking a step further (Herremans 1995; Da Silveira et al., 2016; Brown et al. 2017). As first proposed by Weinzierl et al. (2016) in the field of atmospheric simulation, our study suggests animals are useful sensors and we showed they can also provide valuable ground-truth data for remote sensing-based land cover classification. We mapped agricultural land over three test regions (R1, R2, R3) based on White Stork movement data and achieved high accuracies in R1 and R3. However, we failed in R2 revealing that mapping land cover consistently with animal movement data has its own challenges.

The differences in land management between Central and Western Europe help explain the poor results in R2. According to the Corine Land Cover for 2012, in R1, the agricultural land was dominated by non-irrigated croplands (34%) and grasslands (50%) with no irrigated

 © 2019 The Authors. *Remote Sensing in Ecology and Conservation* published by John Wiley & Sons Ltd on behalf of Zoological Society of London.

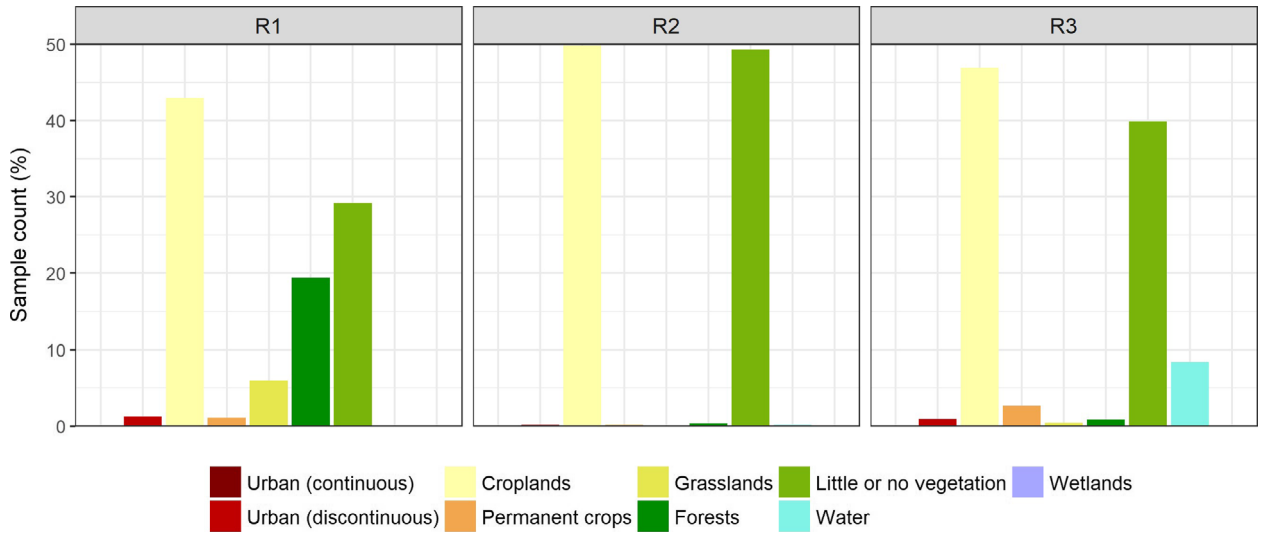

Figure 4. Relative distribution of validation samples per class within each study region.

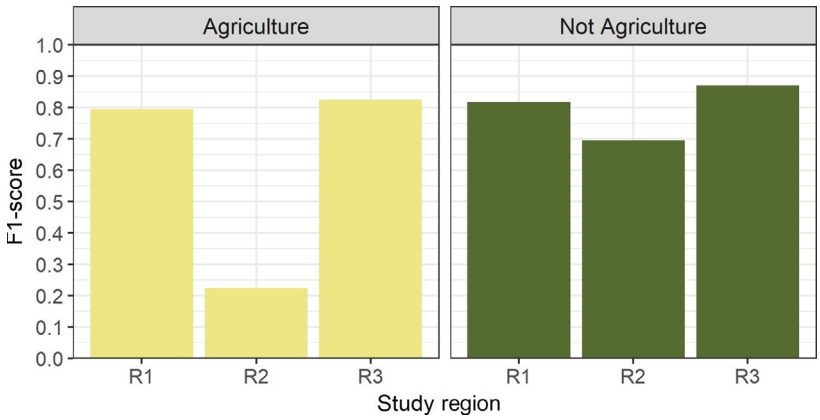

Figure 5. F1-scores for 'Agriculture' and 'Not Agriculture' per study regions.

croplands and a small percentage of permanent crops (2%). However, as we move to R2 and R3, we see a mixture of irrigated and non-irrigated croplands – 38% and 40% in R2 against 40% and 28% in R3 – together with a drastic reduction in managed grasslands – 1% and 6% – and an increase in the proportion of permanent crops such as vineyards – 9% and 3%.

While R2 and R3 were similar, the type of agriculture management sampled in section 2.3 differs among these regions. The percentages of samples over non-irrigated agriculture for R1, R2 and R3 were of 100%, 22% and 45%, respectively, suggesting the White Stork individuals used in this study preferred irrigated land against non-irrigated land when given the choice (Fig. 7). This made it difficult to map the extent of non-irrigated land accurately. The animals showed a similar avoidance for permanent crops justifying our poor performance in mapping this class.

We could address these issues by including data from additional species, particularly specialized foragers attracted by different types of agriculture. For example the common starling (*Sturnus vulgaris*) is infamous among farmers due to the damages they cause to crops (Somers and Morris 2002). However, this is also an advantage when we want to map vineyards and non-irrigated crops (e.g. wheat, corn) where such species forage.

Another issue that might have contributed to the disparities in our results is the temporal coverage of the movement data. As discussed in our previous paper (Remelgado et al. 2018) and done in this study, the differences in temporal and spatial resolution between movement and remote sensing data are addressed by summarizing the movement data into a 'remote sensing friendly' scale that allows for the interoperability of both data. However, while we do address this issue, we are still limited by the date at which the movement data was collected.

© 2019 The Authors. *Remote Sensing in Ecology and Conservation* published by John Wiley & Sons Ltd on behalf of Zoological Society of London.

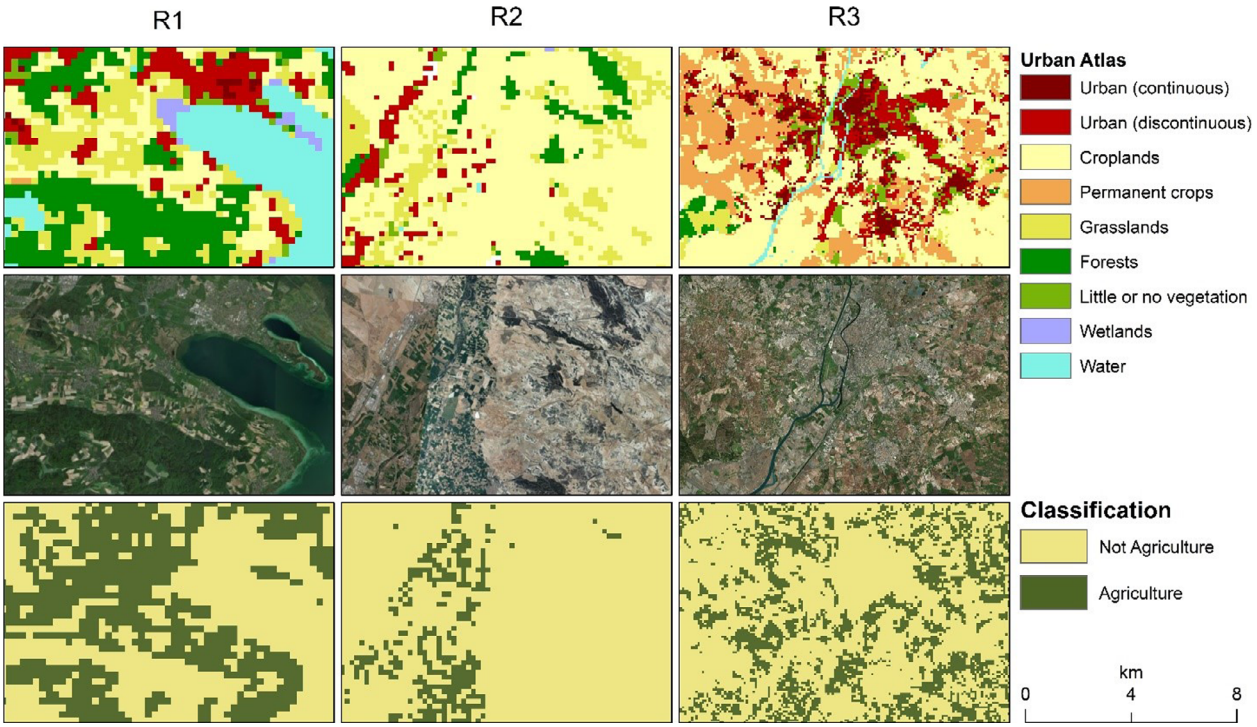

Figure 6. Comparison of UA (top) against the predicted maps (bottom) in each study region.

When mapping agriculture with remote sensing, field experts often visit a sampling site in strategic dates to distinguish seasonal crops. For example winter wheat is planted in the late/early months of the year, whereas maize – which has a similar spectral signature – is planted in late spring and early summer. However, capturing samples from temporally distinct classes through species such as the White Stork can be problematic. The species is sensitive to crop harvesting and planting and takes advantage of open, active fields to prey on species that feed on growing crops (Van Den Bossche 2002; Gordo et al. 2013). Thus, we can miss fields that were at rest during the GPS observation dates.

The observation dates of the movement samples collected in R2 reveal such disparities. Although the samples were collected in August and early September, common,

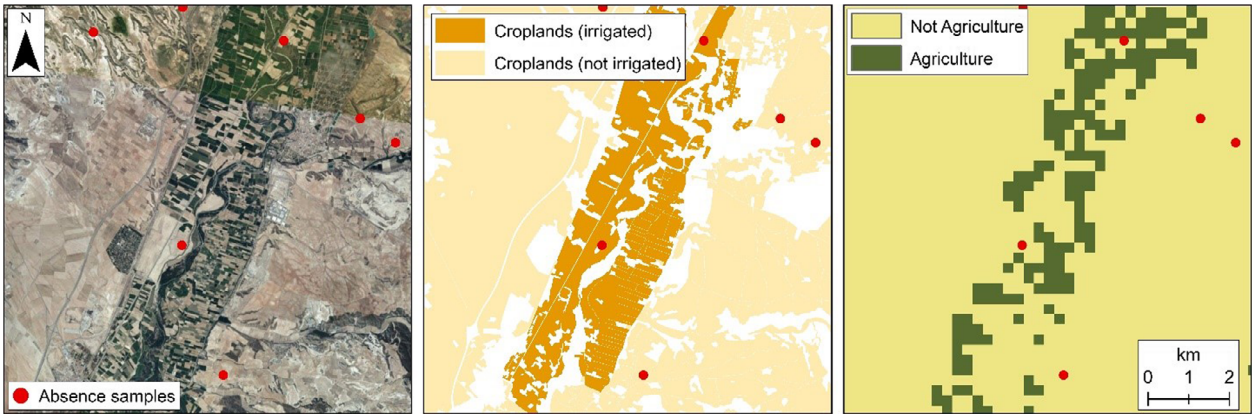

Figure 7. Example from R2 comparing the spatial distribution of irrigated and non-irrigated croplands (center) and the predicted agriculture map (right). 'Arable' land polygons were extracted from UA and relabelled based on their intersection with CLC irrigated and non-irrigated cropland classes.

© 2019 The Authors. *Remote Sensing in Ecology and Conservation* published by John Wiley & Sons Ltd on behalf of Zoological Society of London.

non-irrigated crops such as rye and barley are planted in November–December and harvested in June–July (Gutiérrez Lopez 2013). Combining data from migratory and non-migratory species could address this issue. It would help complement important temporal gaps when the landscape is composed by crops with different growing seasons. However, collecting movement data from multiple species with the same environmental requirements over the same area and over different periods of time can be difficult. As an alternative, semi-automated sampling methods proposed by different authors (Jiang et al. 2012; Mack et al. 2017; Radoux et al. 2014) can be used in combination with movement data from alternate – but similar – locations to complement sampling gaps.

Just as the use of movement data for land cover mapping needs refinement, there are improvements to be made with regards to the use of remote sensing data. Here, the inclusion of satellite-based, multi-spectral information is fairly important. In this paper, we chose to focus on an NDVI time series to map agriculture which, as shown by several authors (Beck et al. 2008; Dong et al. 2016; de Castro et al. 2018; Ghazaryan et al. 2018), describes important phenological traits that help discriminate different types of land management. Moreover, using NDVI data from MODIS, which has a stable temporal and spatial acquisition geometry, assured the consistency of our results across different study regions, making them comparable. However, as shown by other studies (Adam et al. 2010; Selkowitz 2010), multi-spectral information provides an important add-on and helps decipher fuzzy borders between classes and should be considered in fine-scale studies and applications (St-Louis et al. 2014). Moreover, other remote sensing technologies such as Synthetic Aperture Radar (SAR) help discriminate management practices and could reveal useful in improving our results (Inglada et al. 2016; Torbick et al. 2016; Kussul et al. 2018). Yet, few studies combine multi-spectral information with animal movement data (Remelgado et al. 2018) while the use of SAR is non-existent. Therefore, while such technologies have been useful in the scope of traditional land cover mapping, it is still unclear how they will behave in combination with animal movement data, demanding further research.

Although this paper focuses on agriculture, the potential of movement data to map land cover is far reaching. For example existing datasets on barren ground caribou (*Rangifer tarandus groenlandicus*) could provide samples from tundra and grasslands (Rickbeil et al. 2017, 2018), greylag geese (*Anser anser*) could inform us on the existence of permanent – and temporary – water bodies (Kleinhenz and Koenig 2018), and forest elephants (*Loxodonta cyclotis*) could inform us on both grasslands and forests (Mills et al. 2018). To achieve this, we encourage research on the environmental requirements of different species and on the link between these requirements and concrete land cover types. To consolidate this knowledge, initiatives such as MoveBank are a promising source of data (Wikelski and Kays 2019). This online platform allows researchers to share animal tracking data and could be extended by remote sensing experts in support of future, land cover mapping applications.

Once we fully understand the link between animal movement and land cover, animals can provide both training and validation data with a broad spatial and temporal coverage. Animals are not constrained by socio-political boundaries and do not necessarily depend on human infrastructures to move. Moreover, migratory species such as the White Stork have a large mobility while migrating and can travel more than 10 000 km between summer and winter grounds (Flack et al. 2016). With the use of high-resolution, solar-powered GPS trackers, such species can provide frequent information on land cover, and help establish a comprehensive sampling scheme over large areas and over long periods of time.

Still, state-of-the-art movement data can be expensive (Thomas et al. 2011) and its spatial and temporal coverage is often uncertain due to issues such as animal mortality (Hays 2014; Lok et al. 2015). Therefore, while the use of animals as sensors has potential, it does not disregard the value of traditional sampling techniques such as field-campaigns. Instead of investing on movement data as a primary source of samples, researchers and practitioners interested in land cover mapping should view animal movement as complementary data. In this context, including platforms such as MoveBank in the design of field campaigns can help limit their spatial and temporal extent and find data from locations where field campaigns are unfeasible.

Acknowledgements

This research was part of the Opt4Environment project (50 EE 1403) financed by the Federal Ministry for Economic Affairs and Energy (BMWi) through the German Aerospace Agency (DLR). We thank Max Plank's Institute for Ornithology (MPIO) for collecting and providing the movement data used in this study as well as the National Aeronautics and Space Administration (NASA) and the European Space Agency (ESA) for providing the satellite data. Moreover, we specially thank the editor and reviewers for the helpful input, which helped us to improve our paper.

References

Abrahms, B., S. C. Sawyer, N. R. Jordan, J. W. McNutt, A. M. Wilson, and J. S. Brashares. 2017. Does wildlife resource

© 2019 The Authors. *Remote Sensing in Ecology and Conservation* published by John Wiley & Sons Ltd on behalf of Zoological Society of London.

selection accurately inform corridor conservation? *J. Appl. Ecol.* **54**, 412–422

Adam, E., O. Mutanga, and D. Rugege. 2010. Multispectral and hyperspectral remote sensing for identification and mapping of wetland vegetation: a review. *Wetlands Ecol. Manage.* **18**, 281–296

Avgar, T., R. Deardon, and J. M. Fryxell. 2013. An empirically parameterized individual based model of animal movement, perception, and memory. *Ecol. Model.* **251**, 158–172

Beck, P. S. A., T. J. Wang, A. K. Skidmore, and X. H. Liu. 2008. Displaying remotely sensed vegetation dynamics along natural gradients for ecological studies. *Int. J. Remote Sens.* **29**, 4277–4283

Breiman, L. 2001. Random forests. Mach Learn 26.

Brovelli, M. A., I. Celino, A. Fiano, M. E. Molinari, and V. Venkatachalam. 2018. A crowdsourcing-based game for land cover validation. *Applied Geomatics* **10**, 1–11

Brown, M. E. 2016. Remote sensing technology and land use analysis in food security assessment. *Journal of Land Use Science* **11**, 623–641

Brown, L. M., R. K. Fuda, N. Schtickzelle, H. Coffman, A. Jost, A. Kazberouk, et al. 2017. Using animal movement behavior to categorize land cover and predict consequences for connectivity and patch residence times. *Landscape Ecol.* **32**, 1657–1670

de Castro, A., J. Six, R. Plant, and J. Peña. 2018. Mapping crop calendar events and phenology-related metrics at the parcel level by Object-Based Image Analysis (OBIA) of MODIS-NDVI time-series: a Case Study in Central California. *Remote Sens.* **10**, 1745

Da Silveira, N. S., B. B. S. Niebuhr, R. de Lara Muylaert, M. C. Ribeiro, and M. A. Pizo. 2016. Effects of land cover on the movement of frugivorous birds in a heterogeneous landscape. *PLoS ONE* **11**, e0156688.

Didan, K. 2015a. MOD13Q1 MODIS/Terra Vegetation Indices 16-Day L3 Global 250m SIN Grid V006. *NASA EOSDIS Land Processes DAAC*. https://doi.org/10.5067/MODIS/MOD13Q1.006

Didan, K. 2015b. MYD13Q1 MODIS/Aqua vegetation indices 16-Day L3 global 250m SIN Grid V006. *NASA EOSDIS Land Processes DAAC*. https://doi.org/10.5067/MODIS/MYD13Q1.006

Dirmeyer, P. A., D. Niyogi, N. de Noblet-Ducoudré, R. E. Dickinson, and P. K. Snyder. 2010. Impacts of land use change on climate. *Int. J. Climatol.* **30**, 1905–1907

Dodge, S., G. Bohrer, K. Bildstein, S. C. Davidson, R. Weinzierl, M. J. Bechard, et al. 2014. Environmental drivers of variability in the movement ecology of turkey vultures (Cathartes aura) in North and South America. *Philosophical Transactions of the Royal Society B: Biological Sciences* **369**, 20130195–20130195

Dong, J., X. Xiao, M. A. Menarguez, G. Zhang, Y. Qin, D. Thau, et al. 2016. Mapping paddy rice planting area in northeastern Asia with Landsat 8 images, phenology-based algorithm and Google Earth Engine. *Remote Sens. Environ.* **185**, 142–154

European Environment Agency (EEA). 2019. Copernicus Land Monitoring Service [WWW Document]. https://land.copernicus.eu/ accessed 4.12.19.

European Environmental Agency, 2017. The European earth observation Programme — Copernicus land monitoring service. URL http://land.copernicus.eu/ (accessed 3.3.17).

Flack, A., W. Fiedler, J. Blas, I. Pokrovsky, M. Kaatz, M. Mitropolsky, et al. 2016. Costs of migratory decisions: a comparison across eight white stork populations. *Science Advances* **2**, e1500931

Foody, G. M. 2002. Status of land cover classification accuracy assessment. *Remote Sens. Environ.* **80**, 185–201

Foody, G. M. 2004. Supervised image classification by MLP and RBF neural networks with and without an exhaustively defined set of classes. *Int. J. Remote Sens.* **25**, 3091–3104

Fritz, S., L. See, C. Perger, I. McCallum, C. Schill, D. Schepaschenko, et al. 2017. A global dataset of crowdsourced land cover and land use reference data. *Scientific Data* **4**, 170075.

Ghazaryan, G., O. Dubovyk, F. Löw, M. Lavreniuk, A. Kolotii, J. Schellberg, et al. 2018. A rule-based approach for crop identification using multi-temporal and multi-sensor phenological metrics. *European Journal of Remote Sensing* **51**, 511–524

Gordo, O., P. Tryjanowski, J. Z. Kosicki, and M. Fulín. 2013. Complex phenological changes and their consequences in the breeding success of a migratory bird, the white stork *Ciconia ciconia*. *J. Anim. Ecol.* **82**, 1072–1086

Griffith, D., and Y. Chun. 2016. Spatial autocorrelation and uncertainty associated with remotely-sensed data. *Remote Sens.* **8**, 535

Gutiérrez Lopez, M. 2013. Orientaciones varietales para las siembras de cereales en Aragón. Resultado de los ensayos. Cosecha 2013 (No. 252), Informaciones Tecnicas. Dirección General de Alimentación y Fomento Agroalimentario.

Hansen, M. C., and T. R. Loveland. 2012. A review of large area monitoring of land cover change using Landsat data. *Remote Sens. Environ.* **122**, 66–74

Hansen, M. C., P. V. Potapov, R. Moore, M. Hancher, S. A. Turubanova, A. Tyukavina, et al. 2013. High-resolution global maps of 21st-century forest cover change. *Science* **342**, 850–853

Hays, G. C. 2014. Tracking animals to their death. *J. Anim. Ecol.* **83**, 5–6

Herremans, M. 1995. Effects of woodland modification by African elephant Loxodonta africana on bird diversity in northern Botswana. *Ecography* **18**, 440–454

Inglada, J., A. Vincent, M. Arias, and C. Marais-Sicre. 2016. Improved early crop type identification by joint use of high temporal resolution SAR and optical image time series. *Remote Sens.* **8**, 362

 © 2019 The Authors. *Remote Sensing in Ecology and Conservation* published by John Wiley & Sons Ltd on behalf of Zoological Society of London.

Jäger, G., and U. Benz. 2000. Measures of classification accuracy based on fuzzy similarity. *IEEE Trans. Geosci. Remote Sens.* **38**, 1462–1467.

Jia, K., S. Liang, X. Wei, L. Zhang, Y. Yao, and S. Gao. 2014. Automatic land-cover update approach integrating iterative training sample selection and a Markov Random Field model. *Remote Sensing Letters* **5**, 148–156

Jiang, D., Y. Huang, D. Zhuang, Y. Zhu, X. Xu, and H. Ren. 2012. A simple semi-automatic approach for land cover classification from multispectral remote sensing imagery. *PLoS ONE* **7**, 1–11

Kalacska, M., J. Arroyo-Mora, O. Lucanus, and M. Kishe-Machumu. 2017. Land cover, land use, and climate change impacts on endemic cichlid habitats in Northern Tanzania. *Remote Sens.* **9**, 623

Kleinhenz, A., and A. Koenig. 2018. Home ranges and movements of resident graylag geese (Anser anser) in breeding and winter habitats in Bavaria. *South Germany. PLOS ONE* **13**, e0202443

Knorn, J., A. Rabe, V. C. Radeloff, T. Kuemmerle, J. Kozak, and P. Hostert. 2009. Land cover mapping of large areas using chain classification of neighboring Landsat satellite images. *Remote Sens. Environ.* **113**, 957–964

Kussul, N., L. Mykola, A. Shelestov, and S. Skakun. 2018. Crop inventory at regional scale in Ukraine: developing in season and end of season crop maps with multi-temporal optical and SAR satellite imagery. *European Journal of Remote Sensing* **51**, 627–636.

Lang, S., P. Mairota, L. Pernkopf, and E. P. Schioppa. 2015. Earth observation for habitat mapping and biodiversity monitoring. *Int. J. Appl. Earth Obs. Geoinf.* **37**, 1–6.

Liaw, A., and M. Wiener. 2002. Classification and regression by randomforest. *R. News* **2**, 18–22.

Liu, X., G. Hu, Y. Chen, X. Li, X. Xu, S. Li, et al. 2018. High-resolution multi-temporal mapping of global urban land using Landsat images based on the Google Earth Engine Platform. *Remote Sens. Environ.* **209**, 227–239.

Lok, T., O. Overdijk, and T. Piersma. 2015. The cost of migration: spoonbills suffer higher mortality during trans-Saharan spring migrations only. *Biol. Let.* **11**, 20140944.

Lucas, R., P. Blonda, P. Bunting, G. Jones, J. Inglada, M. Arias, et al. 2015. The Earth Observation Data for Habitat Monitoring (EODHaM) system. *Int. J. Appl. Earth Obs. Geoinf.* **37**, 17–28.

Mack, B., P. Leinenkugel, C. Kuenzer, and S. Dech. 2017. A semi-automated approach for the generation of a new land use and land cover product for Germany based on Landsat time-series and Lucas in-situ data. *Remote Sensing Letters* **8**, 244–253.

Mills, E. C., J. R. Poulsen, J. M. Fay, P. Morkel, C. J. Clark, A. Meier, et al. 2018. Forest elephant movement and habitat use in a tropical forest-grassland mosaic in Gabon. *PLoS ONE* **13**, e0199387.

Péron, G., C. H. Fleming, R. C. de Paula, and J. M. Calabrese. 2016. Uncovering periodic patterns of space use in animal tracking data with periodograms, including a new algorithm for the Lomb-Scargle periodogram and improved randomization tests. *Movement Ecology* **4**, 19.

Radoux, J., C. Lamarche, E. Van Bogaert, S. Bontemps, C. Brockmann, and P. Defourny. 2014. Automated training sample extraction for global land cover mapping. *Remote Sens.* **6**, 3965–3987.

Raleigh, C., A. Linke, H. Hegre, and J. Karlsen. 2010. Introducing ACLED: an armed conflict location and event dataset: special data feature. *Journal of Peace Research* **47**, 651–660.

Remelgado, R., B. Leutner, K. Safi, R. Sonnenschein, C. Kuebert, and M. Wegmann. 2018. Linking animal movement and remote sensing – mapping resource suitability from a remote sensing perspective. *Remote Sensing in Ecology and Conservation* **4**, 211–244. https://doi.org/10.1002/rse2.70

Rickbeil, G. J. M., T. Hermosilla, N. C. Coops, J. C. White, and M. A. Wulder. 2017. Barren-ground caribou (Rangifer tarandus groenlandicus) behaviour after recent fire events; integrating caribou telemetry data with Landsat fire detection techniques. *Glob. Change Biol.* **23**, 1036–1047.

Rickbeil, G. J. M., T. Hermosilla, N. C. Coops, J. C. White, M. A. Wulder, and T. C. Lantz. 2018. Changing northern vegetation conditions are influencing barren ground caribou (Rangifer tarandus groenlandicus) post-calving movement rates. *J. Biogeogr.* **45**, 702–712.

See, L., D. Schepaschenko, M. Lesiv, I. McCallum, S. Fritz, A. Comber, et al. 2015. Building a hybrid land cover map with crowdsourcing and geographically weighted regression. *ISPRS J. Photogramm. Remote Sens.* **103**, 48–56.

Selkowitz, D. J. 2010. A comparison of multi-spectral, multi-angular, and multi-temporal remote sensing datasets for fractional shrub canopy mapping in Arctic Alaska. *Remote Sens. Environ.* **114**, 1338–1352.

Shelestov, A., M. Lavreniuk, N. Kussul, A. Novikov, and S. Skakun. 2017. Exploring Google Earth Engine platform for big data processing: classification of multi-temporal satellite imagery for crop mapping. *Frontiers in Earth Science* **5**, 17.

Somers, C. M., and R. D. Morris. 2002. Birds and wine grapes: foraging activity causes small-scale damage patterns in single vineyards. *J. Appl. Ecol.* **39**, 511–523.

St-Louis, V., A. M. Pidgeon, T. Kuemmerle, R. Sonnenschein, V. C. Radeloff, M. K. Clayton, et al. 2014. Modelling avian biodiversity using raw, unclassified satellite imagery. *Philosophical Transactions of the Royal Society B: Biological Sciences* **369**, 20130197–20130197.

Tewkesbury, A. P., A. J. Comber, N. J. Tate, A. Lamb, and P. F. Fisher. 2015. A critical synthesis of remotely sensed optical image change detection techniques. *Remote Sens. Environ.* **160**, 1–14.

© 2019 The Authors. *Remote Sensing in Ecology and Conservation* published by John Wiley & Sons Ltd on behalf of Zoological Society of London.

Thomas, B., J. D. Holland, and E. O. Minot. 2011. Wildlife tracking technology options and cost considerations. *Wildl. Res.* **38**, 653.

van Toor, M. L., S. H. Newman, J. Y. Takekawa, M. Wegmann, and K. Safi. 2016. Temporal segmentation of animal trajectories informed by habitat use. *Ecosphere* **7**, e01498.

Torbick, N., L. Ledoux, W. Salas, and M. Zhao. 2016. Regional mapping of plantation extent using multisensor imagery. *Remote Sens.* **8**, 236.

Van Den Bossche, W. 2002. *Eastern European White Stork Populations: migration Studies and Elaboration of Conservation Measures*. German Federal Agency for Nature Conservation, Bonn.

Vaz, A. S., B. Marcos, J. Gonçalves, A. Monteiro, P. Alves, E. Civantos, et al. 2015. Can we predict habitat quality from space? A multi-indicator assessment based on an automated knowledge-driven system. *Int. J. Appl. Earth Obs. Geoinf.* **37**, 106–113.

Verburg, P. H., O. Mertz, K.-H. Erb, H. Haberl, and W. Wu. 2013. Land system change and food security: towards multi-scale land system solutions. *Curr. Opin. Environ. Sustain.* **5**, 494–502.

Weinzierl, R., G. Bohrer, B. Kranstauber, W. Fiedler, M. Wikelski, and A. Flack. 2016. Wind estimation based on thermal soaring of birds. *Ecol. Evol.* **6**, 8706–8718.

Weiss, D. J., A. Nelson, H. S. Gibson, W. Temperley, S. Peedell, A. Lieber, et al. 2018. A global map of travel time to cities to assess inequalities in accessibility in 2015. *Nature* **553**, 333.

Whitcraft, A., I. Becker-Reshef, and C. Justice. 2015. A framework for defining spatially explicit earth observation requirements for a Global Agricultural Monitoring Initiative (GEOGLAM). *Remote Sens.* **7**, 1461–1481.

Wikelski, M., and R. Kays. 2019. Movebank: archive, analysis and sharing of animal movement data. Hosted by the Max Planck Institute for Ornithology. [WWW Document]. URL www.movebank.org (accessed 4.1.19).

Wulder, M., and B. Boots. 1998. Local spatial autocorrelation characteristics of remotely sensed imagery assessed with the Getis statistic. *Int. J. Remote Sens.* **19**, 2223–2231.

Wulder, M. A., N. C. Coops, D. P. Roy, J. C. White, and T. Hermosilla. 2018. Land cover 2.0. *Int. J. Remote Sens.* **39**, 4254–4284.

Xiong, J., P. S. Thenkabail, M. K. Gumma, P. Teluguntla, J. Poehnelt, R. G. Congalton, et al. 2017. Automated cropland mapping of continental Africa using Google Earth Engine cloud computing. *ISPRS J. Photogramm. Remote Sens.* **126**, 225–244.

Yin, H., A. V. Prishchepov, T. Kuemmerle, B. Bleyhl, J. Buchner, and V. C. Radeloff. 2018. Mapping agricultural land abandonment from spatial and temporal segmentation of Landsat time series. *Remote Sens. Environ.* **210**, 12–24.

Zhao, Y., D. Feng, L. Yu, X. Wang, Y. Chen, Y. Bai, et al. 2016. Detailed dynamic land cover mapping of Chile: accuracy improvement by integrating multi-temporal data. *Remote Sens. Environ.* **183**, 170–185.

Supporting Information

Additional supporting information may be found online in the Supporting Information section at the end of the article.

Data S1: Code guiding trough the proposed data analysis.

 © 2019 The Authors. *Remote Sensing in Ecology and Conservation* published by John Wiley & Sons Ltd on behalf of Zoological Society of London.